Cascade of blind deconvolution and array invariant for robust source-range estimation (L)

H. C. Song[a] and Chomgun Cho
Scripps Institution of Oceanography, La Jolla, California 92093-0238, USA

Gihoon Byun and J. S. Kim
Korea Maritime and Ocean University, Busan, 606-791, South Korea

(Received 29 March 2017; revised 27 April 2017; accepted 28 April 2017; published online 16 May 2017)

The array invariant proposed for robust source localization in shallow water is based on the dispersion characteristics in ideal waveguides. It involves conventional plane-wave beamforming using a vertical array, exploiting multiple arrivals separated in beam angle and travel time, i.e., beam-time migration. The approach typically requires either a short pulse emitted by a source or the Green's function that can be estimated from a probe signal to resolve distinct multipath arrivals. In this letter, the array invariant method is extended to unknown source waveforms by extracting the Green's function via blind deconvolution. The cascade of blind deconvolution and array invariant for robust source-range estimation is demonstrated using a 16-element, 56-m long vertical array at various ranges (1.5–3.5 km) from a towed source broadcasting broadband communication waveforms (0.5–2 kHz) in approximately 100-m deep shallow water. © *2017 Acoustical Society of America*.
[http://dx.doi.org/10.1121/1.4983303]

[ZHM] Pages: 3270–3273

I. INTRODUCTION

The array invariant proposed for source-range estimation in shallow water is based on the dispersion characteristics in ideal waveguides.[1,2] It involves conventional plane-wave beamforming, utilizing multiple arrivals separated in beam angle and travel time, i.e., beam-time migration. The array invariant in the beam-time domain is equivalent to the waveguide invariant in the group- versus phase-velocity domain.[3] To ensure separations of multiple arrivals in time, the approach requires either a strong, short pulse emitted by the source or the Green's function at the receiver array, which is typically obtained from a probe signal such as linear frequency modulation (LFM) chirp by matched-filtering. The array invariant has been successful in achieving robust source-range estimation in shallow-water environments for relatively high-frequency sources (e.g., above 1 kHz) using a probe signal and a vertical line array (VLA), with minimal knowledge of the environment and computational efficiency.[1,4]

The ray-based blind deconvolution that is appropriate for high-frequency signals[5] was developed to estimate both the source waveform and Green's function in a multipath environment from the received signal on the array, which is a convolution of the source signal and Green's function of the propagation medium. The approach also utilizes conventional beamforming that identifies a ray arrival direction to estimate the phase component of the unknown source signal in the frequency domain. The phase contribution of the source signal then can be removed from the received signal, providing an approximate Green's function over the signal bandwidth. Blind deconvolution has been successful in extracting Green's functions from broadband communication signals[5] or ship-generated noise.[6] This letter proposes a combination of blind deconvolution and array invariant, which is applicable to unknown source waveforms for robust source-range estimation.

The paper is organized as follows. In Sec. II, the blind deconvolution and the array invariant are briefly reviewed. To demonstrate the proposed approach, Sec. III describes a recent shallow water experiment conducted in the northeastern East China Sea,[1] with a focus on a broadband source (0.5–2 kHz) broadcasting communication waveforms to a sparse vertical array at various ranges (1.5–3.5 km). A representative Green's function or channel impulse response (CIR) is provided in Sec. IV using the blind deconvolution on a segment of communication waveforms, as compared to the baseline result obtained from the LFM probe in the preamble. The array invariant approach is applied to the estimated Green's function for range estimation in Sec. V, followed by a summary in Sec. VI.

II. BLIND DECONVOLUTION AND ARRAY INVARIANT

A. Blind deconvolution

The theoretical formulation of the blind deconvolution is described in detail in.[5,6] Consider a point source located at $\mathbf{r}_s$ in an acoustic waveguide (see Fig. 1) that broadcasts a signal $s(t)$ whose Fourier transform is $S(\omega) = |S(\omega)|e^{i\Phi_s(\omega)}$. The Fourier transform of the received signal $p_j(t)$ on the jth element of the array located at $\mathbf{r}_j$ is given by

$$P_j(\omega) = G(\mathbf{r}_j, \mathbf{r}_s, \omega)S(\omega), \tag{1}$$

where $G(\mathbf{r}_j, \mathbf{r}_s, \omega)$ is the Fourier transform of the Green's function $g(\mathbf{r}_j, \mathbf{r}_s, t)$ between the source and jth element of the VLA ($1 \le j \le N$).

[a]Electronic mail: hcsong@ucsd.edu

 0001-4966/2017/141(5)/3270/4/$30.00

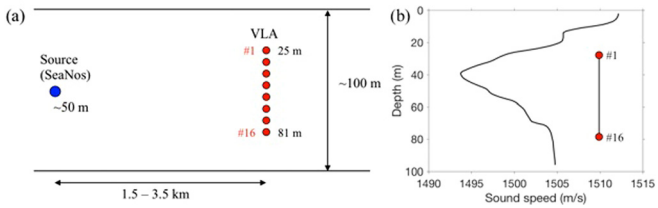

FIG. 1. (Color online) (a) Schematic of a source-tow run on JD 146 (May 26). A 16-element vertical line array (VLA) was moored in 100-m deep water. A broadband source (0.5–2 kHz) deployed to 50 -m depth was towed at a radial speed of approximately 2 m/s at various ranges (1.5–3.5 km). (b) SSP averaged from three CTD profiles collected around JD 146, featuring an asymmetrical underwater sound channel (USC) with the channel axis at 40 m.

The first step is to apply a conventional delay-and-sum beamformer in a specific beam direction θ that is defined with respect to the horizontal (i.e., grazing angle), whose output $B(\omega, \theta)$ is expected to capture the source signal and its phase component $\Phi_s(\omega)$:

$$B(\omega,\theta) = \sum_{j=1}^{N} \exp\{-i\omega\tau(\theta,\mathbf{r}_j)\}P_j(\omega) \approx |B(\omega,\theta)|\exp\{i\Phi_s(\omega) - i\omega T(\theta)\}, \quad (2)$$

where $\tau(\theta, \mathbf{r}_j)$ is the local time delay at the jth element with respect to a reference position (e.g., array center)[7] and $T(\theta)$ is the ray travel time from the source to the receiver array.

Given the phase of the beamformer output, $\phi(\omega,\theta) = \Phi_s(\omega) - \omega T(\theta)$, the key to ray-based blind deconvolution is a removal of the unknown source phase component $\Phi_s(\omega)$ from the received data vector $P_j(\omega)$ simply by a phase-rotation:

$$\hat{G}(\mathbf{r}_j,\mathbf{r}_s,\omega) = P_j(\omega)\exp\{-i\phi(\omega,\theta)\} = |S(\omega)|G(\mathbf{r}_j,\mathbf{r}_s,\omega)\exp\{i\omega T(\theta)\}. \quad (3)$$

The resulting array output, denoted by $\hat{G}(\mathbf{r}_j, \mathbf{r}_s, \omega)$, provides an estimate of the Green's function up to a linear frequency shift $\omega T(\theta)$, which corresponds to a time delay of $T(\theta)$. The amplitude shading term $|S(\omega)|$ can be easily eliminated by pre-normalization of the received signal $P_j(\omega)$,[8] or can be neglected when the source signal is white (i.e., spectrally flat) such as phase-coherent communication waveforms that will be used in this paper.

B. Array invariant

The array invariant derived in[1,3] can be applied to the Green's function estimated by the blind deconvolution. The horizontal distance between the source and receiver (r_0) can be obtained simply from

$$r_0 = -\beta\left(\frac{c}{\chi}\right), \quad (4)$$

where β is the waveguide invariant[9] and c is the local sound speed used for beamforming. For an ideal waveguide and most bottom-interacting shallow-water environments, $\beta \approx 1$, and this formula reduces to the original array invariant.[2]

The array invariant parameter χ is defined as

$$\chi \equiv \frac{d}{dt}(\cos\theta) = \frac{d}{dt}\sqrt{1-\sin^2\theta} = \frac{d}{dt}\sqrt{1-s^2}, \quad (5)$$

where $s = \sin\theta$ and t is the travel time. The above equation leads to an elliptic curve in the beam-time (s, t) coordinate (see Fig. 4):

$$\left(\frac{t-t_0}{1/\chi}\right)^2 + \sin^2\theta = 1, \quad (6)$$

whose center is located at (0, t_0) and $1/|\chi|$ is the horizontal semi-major axis.[3] The parameter χ can be estimated numerically from the beam-time migration data, e.g., using the least-squares (LS) approach as described in the Appendix of Ref. 1.

III. SAVEX15 EXPERIMENT

The shallow-water acoustic variability experiment (SAVEX15) was conducted in the northeastern East China Sea during May 2015.[1] The experimental site had a nearly flat sandy bottom and water depth of approximately 100 m. Both fixed and towed source transmissions were carried out to two moored vertical line arrays (VLAs) over ranges of 1–10 km. The acoustic transmissions were in various frequency bands covering 0.5−32 kHz and included both channel probing waveforms as well as communication sequences. Environmental data included water column sound speed structure, sea surface directional wave field, and local wind speed and direction.

To investigate the blind deconvolution for Green's function estimation and array invariant for source-range estimation, we revisit the dataset analyzed in Ref. 1 during a source-tow run conducted on JD 146 (May 26), from 16:40 to 16:55 UTC. The schematic of the source-tow run is illustrated in Fig. 1(a). A broadband source (0.5–2 kHz) called SeaNos was deployed to about 50 -m depth and towed by the R/V Onnuri mostly at a speed of 4 knots (2 m/s) along a specified ship track. The source level (SL) was modest with 165 dB re μPa at 1 m. The VLA consisted of 16 elements spanning a 56.25-m aperture with 3.75-m element spacing, covering about half the water column (from 25 to 81 m) in about 100-m deep water.

A sound speed profile (SSP) averaged from three CTD (conductivity, temperature, and depth) casts conducted before and after the source-tow run is shown in Fig. 1(b). Surprisingly, the SSP indicates an underwater sound channel (USC) that is typical for deep water, although a similar USC is also observed during the summer in the shallow southern Baltic Sea.[10] The USC is asymmetric with respect to the channel axis at 40 m close to the source depth (50 m). The variation of the sound speed across the VLA [Fig. 1(b)] is about 12 m/s.

IV. ESTIMATION OF GREEN'S FUNCTION

In this section, a representative Green's function is estimated using a LFM channel probe and then blind deconvolution for comparison purposes.

A. LFM probe

A typical communication data packet transmitted during the source-tow run is shown in Fig. 2(a), comprised of a 100-ms long LFM chirp (0.5–2 kHz) followed by a 5-s long communication sequence that is encoded with an assortment of modulations and data rate.[11] The LFM probe in the preamble can be used for both channel synchronization and CIR estimation purposes. As a baseline, the Green's function (or CIR) estimated at 1.5 km range using the LFM probe is displayed in Fig. 3(a) along the VLA depth after matched-filtering (JD146165540). The horizontal axis is a relative travel time (ms) with the high-intensity arrival placed at $t = 0$ ms. The arrival structure appears complicated with many distinct paths and a delay spread of up to 70 ms, indicating a reverberant acoustic environment. While the modest source level (165 dB) was compensated for by the pulse compression gain of about 22 dB, Fig. 2(a) shows that its peak level is only about 10 times larger than the root-mean-square amplitude of the communication waveform that follows.

B. Blind deconvolution

Now we turn to blind deconvolution and select a 4-s long communication waveform, denoted by a rectangular box in Fig. 2(a). The communication sequence is phase-coherent with a raised cosine filter and thus can be assumed spectrally white over the bandwidth.[11] A conventional beamforming applied to the selected waveforms in the frequency domain is displayed in Fig. 2(b), averaged over the frequency band (0.5–2 kHz), with a positive beam angle representing an up-going ray path. The dominant angle of arrival is about $\theta = 4.2°$, which corresponds to the high-intensity blob (red) at around $t = 0$ ms in Fig. 3(a). They are from low-order, refracted modes whose energy is trapped around the

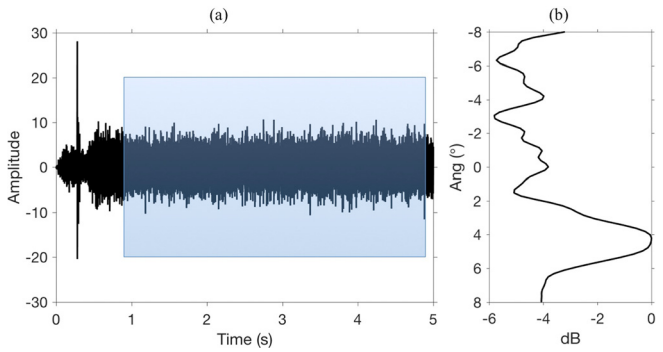

FIG. 2. (Color online) (a) Typical 5-s long communication sequence that includes a 100-ms, 0.5–2 kHz LFM chirp probe in the preamble received by a single element of the VLA (located at the depth of 50 m). The received signal is matched-filtered by the LFM probe with its peak at around $t = 0.2$ s. The Green's function from the LFM probe is presented in Fig. 3(a) as a baseline. The rectangular box denotes a 4-s long communication waveform selected across the VLA, which are used for blind deconvolution to estimate the Green's function presented in Fig. 3(b). (b) Conventional beamforming of the selected waveforms in the frequency domain averaged over the frequency band (0.5–2 kHz), with a positive angle representing an up-going ray path. The dominant angle of arrival is about $\theta = 4.2°$, which is associated with high-intensity, low-order refracted modes trapped in the USC that stand out in Fig. 3 as a red blob around $t = 0$. Blind deconvolution involves steering the beam to the direction ($\theta = 4.2°$) in order to capture the source waveform and estimate the unknown source phase $\Phi_s(\omega)$ in Eq. (2).

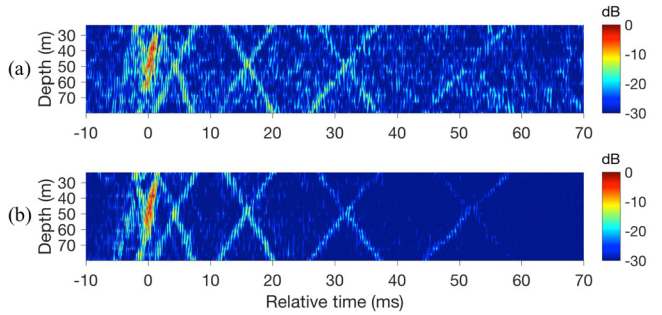

FIG. 3. (Color online) Green's function (or CIR) estimated at 1.5 km range (JD146165540) from: (a) LFM channel probe after matched-filtering and (b) blind deconvolution of the selected 4-s waveform in Fig. 2(a) (rectangular box). While the overall agreement between the two is excellent in terms of the arrival structure, (b) blind deconvolution outperforms (a) LFM probe with a lower background level (ambiguity) and an improved resolution of individual ray paths, in particular at around $t = 0$. The six X-shaped distinct arrivals captured between 0 and 40 ms are exploited for source-range estimation based on the array invariant method.

channel axis (40 m), excited by the source at 50-m depth being close to the channel axis.[1] To estimate the unknown source phase $\Phi_s(\omega)$ in Eq. (2), blind deconvolution involves steering the beam to the direction ($\theta = 4.2°$).

The Green's function obtained using blind deconvolution is presented in Fig. 3(b), in parallel with the baseline result in Fig. 3(a). The overall agreement between the two appears excellent in terms of the arrival structure and confirms that blind deconvolution can be a surrogate for a channel probe in extracting the Green's function.[5] What is remarkable is that (b) blind deconvolution outperforms (a) LFM probe with a lower background noise level (ambiguity) and an improved resolution of individual ray paths, especially around $t = 0$ where the high-intensity arrival propagating upward (red blob) is visible with clarity.

The enhancement of the Green's function indicates that blind deconvolution can make an effective use of the energy carried by the 4-s long waveform over the short 100-ms long LFM probe signal for a modest source level (165 dB). In addition, the blind deconvolution benefited from the beam steered to the refracted modes ($\theta = 4.2°$) that did not interact with boundaries, allowing for a minimally distorted source waveform to be captured in Eq. (2). Although not shown here, we have examined the Green's function at two other ranges (2.8 and 3.5 km) and found a similar performance improvement with blind deconvolution.

V. BEAM-TIME MIGRATION

For source-range estimation, the beam-time migration (s, t) is presented in Fig. 4 in grayscale: (a) LFM probe and (b) blind deconvolution, each corresponding to Fig. 3, respectively. The vertical axis represents the beam angle ($s = \sin\theta$) with a positive value defined for an up-going path (e.g., red circles), and the horizontal axis is the relative travel time t (ms). The VLA is positioned around the channel axis with significant variation of the sound speed up to 12 m/s [refer to Fig. 1(b)] and thus an averaged sound speed of $c = 1500$ m/s is used for plane-wave beamforming. Although the design frequency for the VLA is 200 Hz with the element

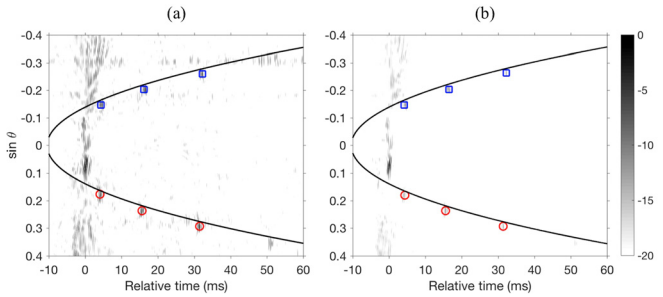

FIG. 4. (Color online) Beam-time migration at 1.5 km range: (a) LFM probe and (b) blind deconvolution, each corresponding to Fig. 3. A positive beam angle represents an up-going ray path (e.g., red circles) and the dynamic range is 20 dB. Despite the similarities, the ambiguities (sidelobes) are noticeably reduced for (b) blind deconvolution. The high-intensity arrivals around $t = 0$ ms are from refracted low-order modes that are confined to the broadside (e.g., $|\sin\theta| < 0.1$), whereas the similar structure appearing on both sides at higher angles ($|\sin\theta| > 0.2$) is due to spatial aliasing. The six reflected arrivals, marked by circles and squares between 0 and 40 ms, constitute an elliptic curve (solid line) from which the array invariant parameter χ can be obtained for source-range estimation. The estimated source range is 1.6 km with a relative error of 7% in both cases.

spacing of 3.75 m, the spatial aliasing in beam angle (i.e., grating lobes) is mitigated over the broad frequency band (0.5–2 kHz). The dynamic range is 20 dB.

Several observations can be made as follows. While there is an excellent agreement between the two, sidelobes (ambiguities) are reduced significantly in (b) blind deconvolution. This is not surprising given the enhancement of the Green's function shown in Fig. 3. Second, the early high-intensity arrivals around $t = 0$ ms are spread around the broadside (i.e., $|s| < 0.1$), a contribution from refracted low-order modes with smaller grazing angles. The similar, less-intense (e.g., 7 dB below) structure appearing on both sides at higher angles ($|s| > 0.2$) is due to spatial aliasing with the sparse VLA. Third, many reflected arrivals at higher angles ($0.1 < |s| < 0.3$) are visible, albeit weak, marked by circles and squares. For array invariant-based range estimation, the six distinct arrivals of up- (circles) and down-going (squares) rays captured between 0 and 40 ms are exploited.

Finally, an elliptic curve (solid line) corresponding to Eq. (5) that best fits the six reflected arrivals (circles and squares) in the least-squares sense is obtained with an appropriate array invariant parameter χ, enabling the source-range estimation based on Eq. (4). Note that the distinct arrivals in Fig. 4 are a little offset from the elliptic curve by approximately 0.7° likely due to an array tilt, which is neglected in this paper. However, the impact of array tilt on the array invariant is analyzed in Ref. 12. The estimated source range is 1.6 km with a relative error of about 7% in both cases. For two other ranges (2.8 and 3.5 km), the blind deconvolution resulted in a similar or better performance, which is summarized in Table I.

TABLE I. Source-range estimation based on beam-time migration of the Green's function obtained at various ranges using (a) LFM probe and (b) blind deconvolution.

Source range	(a) LFM probe		(b) Blind deconvolution	
	Estimated range	Relative error	Estimated range	Relative error
1.5 km	1.6 km	7%	1.6 km	7%
2.8 km	3.2 km	15%	3.1 km	14%
3.5 km	4.1 km	17%	4.0 km	13%

VI. SUMMARY

The array invariant proposed for robust source localization in shallow water is based on the dispersion characteristics in ideal waveguides. It involves conventional plane-wave beamforming using a vertical array, exploiting multiple arrivals separated in beam angle and travel time. Thus the approach requires either a strong, impulsive source or knowledge of the Green's function typically obtained using a probe signal. In this letter, the array invariant was extended to unknown source waveforms by extracting the Green's function via blind deconvolution. It was found that the blind deconvolution using a longer waveform (e.g., 4-s) can provide a better estimate of the Green's function over the short (100-ms) LFM probe signal for a modest source (165 dB). The cascade of blind deconvolution and array invariant for robust source-range estimation is demonstrated using a 16-element, 56-m long vertical array at various ranges (1.5–3.5 km) from a towed source broadcasting broadband communication waveforms (0.5–2 kHz) in approximately 100 -m deep shallow water.

ACKNOWLEDGMENT

This research was supported by the U.S. Office of Naval Research.

[1]H. C. Song and C. Cho, "Array invariant-based source localization in shallow water using a sparse vertical array," J. Acoust. Soc. Am. **141**, 183–188 (2017).
[2]S. Lee and N. C. Makris, "The array invariant," J. Acoust. Soc. Am. **119**, 336–351 (2006).
[3]H. C. Song and C. Cho, "The relation between the waveguide invariant and array invariant," J. Acoust. Soc. Am. **138**, 899–903 (2015).
[4]C. Cho, H. C. Song, and W. S. Hodgkiss, "Robust source-range estimation using the array/waveguide invariant and a vertical array," J. Acoust. Soc. Am. **139**, 63–69 (2016).
[5]K. Sabra, H. Song, and D. Dowling, "Ray-based blind deconvolution in ocean sound channels," J. Acoust. Soc. Am. **127**, EL42–EL47 (2010).
[6]S. Byun, C. Verlinden, and K. Sabra, "Blind deconvolution of shipping sources in an acoustic waveguide," J. Acoust. Soc. Am. **141**, 797–807 (2017).
[7]M. Dzieciuch, P. Worcester, and W. Munk, "Turning point filters: Analysis of sound propagation on a gyre-scale," J. Acoust. Soc. Am. **110**, 135–149 (2001).
[8]K. Sabra and D. R. Dowling, "Blind deconvolution in ocean waveguides using artificial time reversal," J. Acoust. Soc. Am. **116**, 262–271 (2004).
[9]F. B. Jensen, W. A. Kuperman, M. B. Porter, and H. Schmidt, *Computational Ocean Acoustics* (Springer, New York, 2011), Chaps. 3 and 5.
[10]G. Grelowska, "Prevailing patterns of the sound speed distributions in the environment of the southern Baltic," Arch. Acoust. **25**, 359–368 (2000).
[11]H. C. Song, "An overview of underwater time-reversal communication," IEEE J. Ocean. Eng. **41**, 644–655 (2016).
[12]C. Cho and H. C. Song, "Impact of array tilt on source-range estimation in shallow water using the array invariant," J. Acoust. Soc. Am. **141**, 2849–2856 (2017).